Outlier detection for high b-value diffusion data

Kerstin Pannek[1], David Raffelt[2], Christopher Bell[1], Jane Mathias[3], and Stephen Rose[1]

[1]The University of Queensland, Brisbane, Queensland, Australia, [2]Brain Research Institute, Australia, [3]University of Adelaide, Australia

Introduction: Diffusion-weighted (DW) images are prone to artefacts caused by physiological noise, such as head movement and cardiac pulsation. These artefacts are typically observed as signal dropout. The RESTORE method (Robust EStimation of Tensors by Outlier REjection, [1]) was proposed to identify voxels and directions with outlier intensities. RESTORE, however, uses the diffusion tensor model for outlier detection. As the diffusion tensor cannot appropriately model more than a single fibre population, identification of outlier voxels in crossing fibre regions may be inaccurate, particularly when diffusion data is acquired at high b-values required for higher order models. We hypothesized that an increased number of outlier voxels would be observed in crossing fibre areas using RESTORE. To overcome this limitation, we developed HOMOR (Higher Order Model Outlier Rejection), which is closely related to the RESTORE method, but employs a higher order model capable of resolving multiple fibre populations within a single voxel.

Methods: For this study, we fit the DW signal using spherical harmonics at a maximum harmonic degree 4 (i.e. fitting 15 parameters). We reject outliers from the SH model based on the assumption that DW signal should vary smoothly as a function of orientation and not contain angular frequencies that would cause the SH model to have residuals larger than 3 times the signal standard deviation. Outlier voxels were identified in the individual DW volumes using an iterative process, based on the residuals computed between the SH model and the DW data. Voxels with residuals larger than 3 times the signal standard deviation were considered outliers and excluded from the subsequent iteration. The process was repeated until convergence was achieved. The workflow is summarized in Figure 1.

To investigate the proposed method, data from 103 healthy participants (54 male, age 18-73 years) were analysed. Diffusion MRI data were acquired without cardiac gating along 64 non-collinear directions at b = 3000 s/mm^2 and 2.5 mm isotropic resolution using a 3T scanner. Data preprocessing included correction for head movement, susceptibility distortions and intensity inhomogeneity. FA maps were calculated and registered non-linearly to a study-specific FA template using the ANTS software package and an iterative update approach. Outlier voxels were identified in diffusion space using RESTORE and HOMOR. The signal standard deviation was calculated directly from the residuals as described in [2], using the assumption that less than half of all brain voxels are affected by artefacts. Outlier Rejection Probability maps (ORP) were calculated for every participant as described previously [2]: for every voxel, the number of outliers was recorded and normalized using the number of degrees of freedom (degrees of freedom = number of directions – number of fit parameters).

Figure 1: Workflow for outlier detection

ORPs were transformed to the template space using the non-linear transformation obtained from the FA-estimated warps, and averaged across all participants. Additionally, FA maps and FOD images (estimated using constrained spherical deconvolution [3], harmonic degree 8) were computed from the original DW data, as well as data output from both RESTORE and HOMOR. FA and FOD images were then spatially normalised using the FA computed warps. FODs were reoriented during spatial normalisation using apodised point spread functions [4]. Population variability (coefficient of variation, CV) of the FA and FOD images was calculated in template space, and compared between the different methods of outlier rejection. Note that for FOD images, the CV of the FOD amplitude was computed as the median CV over 300 equally distributed directions.

Figure 3: Average outlier rejection probability (ORP) maps obtained using RESTORE and HOMOR. The ORP on the right indicates areas where RESTORE and HOMOR consistently identified outliers. All images are shown using the same windowing.

Results: Figure 2 shows average Outlier Rejection Probability maps obtained using RESTORE and HOMOR. A large number of outliers were detected in crossing fibre regions (e.g. corona radiata – red circle in Figure 2) when RESTORE (tensor model) was used. However, no significant number of outliers were identified in these regions using HOMOR. A number of other regions were identified consistently for both methods, including the splenium of the corpus callosum, brainstem, cerebellum, as well as areas prone to susceptibility distortions in the frontal and temporal lobes. When RESTORE was used for outlier detection, an increase in population variability of FA was observed in crossing fibre areas, as well as in single fibre areas (Figure 3). FOD population variability was increased within crossing fibre regions with RESTORE. Slight increases in FA population variability were observed when HOMOR was used for outlier detection, but no trends were observed in FOD population variability with HOMOR.

Discussion: Our results show that if RESTORE is used in high b-value data, a large number of voxels within crossing fibre areas are incorrectly identified as outliers. Excluding these voxels from subsequent analysis may introduce a bias in the estimated fibre orientation and quantitative metrics (e.g. FA). In contrast, using a higher order model for outlier rejection identified outlier voxels mainly within areas prone to cardiac pulsation artefacts and susceptibility distortions.

Figure 2: Population variability increase (red-yellow) and decrease (blue-cyan) of FA (top) and FOD (bottom) after outlier rejection using RESTORE (left) and HOMOR (right).

References:
[1] Chang et al., 2005. Magn Reson Med 53(5): 1088-1095. [2] Walker et al., 2011. Neuroimage 54(2): 1168-1177. [3] Tournier et al., 2007. Neuroimage 35(4): 1459-1472. [4] Raf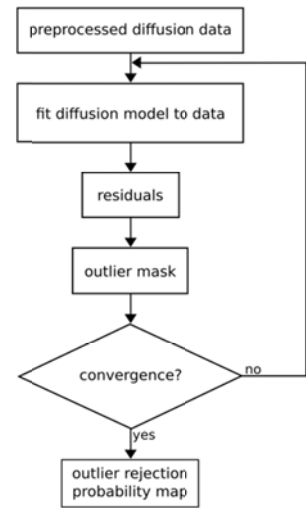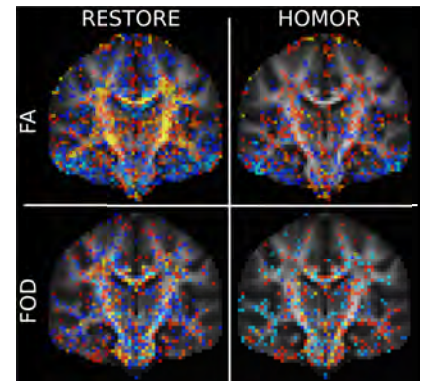felt et al., 2011. Neuroimage 56(3): 1171-1180